ELSEVIER

Journal of Hazardous Materials 141 (2007) 520–528

Journal of Hazardous Materials

www.elsevier.com/locate/jhazmat

UV light induced photodegradation of malachite green on TiO_2 nanoparticles

C.C. Chen [a,*], C.S. Lu [a], Y.C. Chung [b], J.L. Jan [a]

[a] *Department of General Education, National Taichung Nursing College, Taichung 403, Taiwan*
[b] *Department of Biological Science and Technology, China Institute of Technology, Taipei 115, Taiwan*

Received 23 January 2006; received in revised form 29 June 2006; accepted 10 July 2006
Available online 14 July 2006

Abstract

The photodegradation of malachite green (MG), a cationic triphenylmethane dye, is examined both under different pH values and amounts of TiO_2. After 15 W UV-365 nm irradiation for 4 h, ca. 99.9% of MG was degraded with addition of 0.5 g L^{-1} TiO_2 to solutions containing 50 mg L^{-1} of the MG dye. The HPLC–PDA–ESI-MS technique was used to obtain a better understanding on the mechanistic details of this TiO_2-assisted photodegradation of the MG dye with UV irradiation. Five intermediates of the process were separated, identified, and characterized for the first time. The results indicated that the *N*-de-methylation degradation of MG dye took place in a stepwise manner to yield mono-, di-, tri-, and tetra-*N*-de-methylated MG species generated during the processes. Under acidic conditions, the results indicated that the photodegradation mechanism is favorable to cleavage of the whole conjugated chromophore structure of the MG dye. Under basic conditions, the results showed that the photodegradation mechanism is favorable to a formation of a series of *N*-de-methylated intermediates of the MG dye.

Keywords: Malachite green; Dye; Photodegradation; TiO_2; *N*-De-methylation

1. Introduction

In the past decade, TiO_2-mediated photocatalysis has been successfully used to degrade pollutants [1–5]. TiO_2 is broadly used as a photocatalyst because of its non-toxicity, photochemical stability, and low cost [4,5]. The initial step in the TiO_2-mediated photocatalysis degradation is proposed to involve the generation of a (e^-/h^+) pair leading to the formation of hydroxyl radicals ($^\bullet OH$), superoxide radical anions ($O_2^{\bullet -}$), and hydroperoxyl radicals ($^\bullet OOH$), and these radicals are the oxidizing species in the photocatalytic oxidation processes. The efficiency of the dye degradation depends on the concentration of the oxygen molecules, which either scavenge the conduction band electrons (e_{cb}^-) or prevent the recombination of (e^-/h^+). The electron in the conduction band can be picked up by the adsorbed dye molecules, leading to the formation of dye radical anions and the degradation of the dye [5].

The chemical structure of this MG dye is shown in Fig. 1. It is an extensively used biocide in the global aquaculture industry, and is highly effective against important protozoal and fungal infections [6,7]. Essentially, it works as an ectoparasiticide and has been used to control skin flukes and gill flukes. Aquaculture industries have been using malachite green extensively as a typical treatment by bath or flush methods without regard for the fact that topically applied therapeutants might also be absorbed systemically and produce significant internal effects. On the other hand, it is also used as a food coloring agent, food additive, medical disinfectant, and anthelminthic as well as a dye in the silk, wool, jute, leather, cotton, paper, and acrylic industries [8]. However, malachite green has now become a highly controversial compound due to the risks it poses to the consumers of treated fish [9,10], including its effects on the immune system and reproductive system and its genotoxic and carcinogenic properties [11]. Though the use of this dye has been banned in several countries and is not approved by US Food and Drug Administration, it is still being used in many parts of the world due to its low cost, ready availability, and efficacy [6]. A considerable amount of research is being devoted to the wide spectrum of biological effects it exerts on different animals and

* Corresponding author. Tel.: +886 4 2219 6975; fax: +886 4 2376 0579.
E-mail address: ccchen@ntcnc.edu.tw (C.C. Chen).

0304-3894/$ – see front matter © 2006 Elsevier B.V. All rights reserved.
doi:10.1016/j.jhazmat.2006.07.011

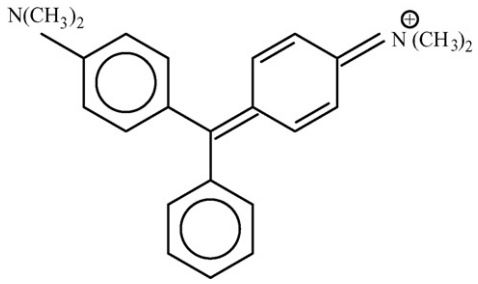

Fig. 1. Chemical structure of malachite green.

on mankind. The US Food and Drug Administration has nominated MG as a priority chemical for carcinogenicity testing. There is concern about the fate of MG and its reduced form, leucomalachite green in aquatic and terrestrial ecosystems science they occur as contaminants and are potential human health hazards [12].

In earlier reports [13–15], the photodegradation of malachite green (CI 42,000) was investigated. Most studies have focused on new photocatalysts, the effects of experimental conditions, and the possibility of environmental application, not on decomposed mechanisms and intermediates. However, the photodegradation intermediates of this dye have not been isolated or identified.

Accordingly, these studies focused on the identification of the reaction intermediates and throw some light on the mechanistic details of the photodegradation of MG dye in the P-25 TiO_2/UV process by HPLC–PDA–ESI-MS. Additionally, the effects of TiO_2 dosage and pH on the degradation rate of the dyes were measured.

2. Materials and methods

2.1. Materials

The TiO_2 photocatalyst (P25, ca. 80% anatase, 20% rutile; particle size, ca. 20–30 nm; BET area, ca. 55 $m^2\,g^{-1}$) was kindly supplied by Degussa. MG (bis[*p*-dimethylaminophenyl]phenylmethylium oxalate) dye was obtained from Tokyo Kasei Kogyo Co. and used without any further purification. Stock solutions containing 1 $g\,L^{-1}$ of MG dye in water were prepared, protected from light, and stored at 4 °C. HPLC analysis was employed to confirm the presence of the MG dye as a pure organic compound.

Reagent-grade ammonium acetate, sodium hydroxide, nitric acid, and HPLC-grade methanol were purchased from Merck. De-ionized water was used throughout this study. The water was then purified with a Milli-Q water ion-exchange system (Millipore Co.) to give a resistivity of $1.8 \times 10^7\ \Omega$ cm.

2.2. Instruments

A Waters ZQ LC/MS system, equipped with a binary pump, a photodiode array detector, an autosampler, a frational collector, and a micromass detector, was used for separation and identification. The C-75 Chromato-Vue cabinet of UVP provides a wide area of illumination from the 15-W UV-365 nm tubes positioned on two sides of the cabinet interior.

2.3. Procedures and analysis

An aqueous TiO_2 dispersion was prepared by adding 50 mg of TiO_2 powder to a 100 mL solution containing the MG dye at appropriate concentrations. For reactions in different pH media, the initial pH of the suspensions was adjusted by addition of either NaOH or HNO_3 solutions. Prior to irradiation, the dispersions were magnetically stirred in the dark for ca. 30 min to ensure the establishment of adsorption/desorption equilibrium. Irradiations were carried out using two UV-365 nm lamps (15 W). At any given irradiation time interval, the dispersion was sampled (5 mL), centrifuged, and subsequently filtered through a Millipore filter (pore size, 0.22 μm) to separate the TiO_2 particles.

After each sampled cycle, the amount of the residual dye was thus determined by HPLC. The analysis of organic intermediates was accomplished by HPLC–ESI-MS after the readjustment of the chromatographic conditions in order to make the mobile phase compatible with the working conditions of the mass spectrometer. Two different kinds of solvents were prepared in this study. Solvent A was 25 mM aqueous ammonium acetate buffer (pH 6.9) while solvent B was methanol instead of ammonium acetate. LC was carried out on an Atlantis^{TM} dC18 column (250 mm × 4.6 mm i.d., dp = 5 μm). The flow rate of the mobile phase was set at 1.0 mL/min. A linear gradient was set as follows: $t = 0, A = 95, B = 5$; $t = 20, A = 50, B = 50$; $t = 40$–$45, A = 10, B = 90$; $t = 48, A = 95, B = 5$. The column effluent was introduced into the ESI source of the mass spectrometer.

Equipped with an ESI interface, the quadruple mass spectrometer with heated nebulizer probe at 350 °C was used with an ion source temperature of 80 °C. ESI was carried out with the vaporizer at 350 °C and nitrogen as sheath (80 psi) and auxiliary (20 psi) gas to assist with the preliminary nebulization and to initiate the ionization process. A discharge current of 5 μA was applied. Tube lens and capillary voltages were optimized for the maximum response during perfusion of the MG standard.

Performed in flasks without the addition of TiO_2, the blank experiments show no appreciable decolorization of the irradiated solution, thus confirming the expected stability of MG dye under UV light irradiation. Also, with addition of 0.5 $g\,L^{-1}$ TiO_2 to solutions containing 50 mg L^{-1} of the MG dye, the stability of the dye did not alter in the dark either.

3. Results and discussion

3.1. pH effect

In an aqueous system, TiO_2 is amphoteric [16]. The TiO_2 surface is predominantly negatively charged when the pH is higher than the TiO_2 isoelectric point. As the pH decreases, the functional groups are protonated, and the proportion of the positively charged surface increases. Thus, the electrical property of the TiO_2 surface varies with the pH of the dispersion. The surface of TiO_2 would be negatively charged and adsorb cationic species

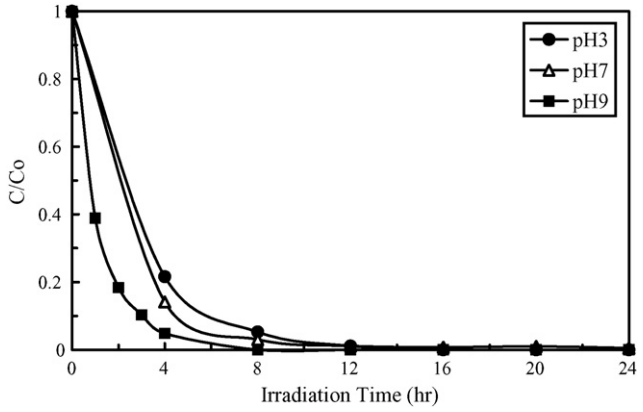

Fig. 2. pH effect on the MG photodegradation rate with concentrations of TiO_2 to be 0.5 g L^{-1} and MG to be 0.05 g L^{-1}.

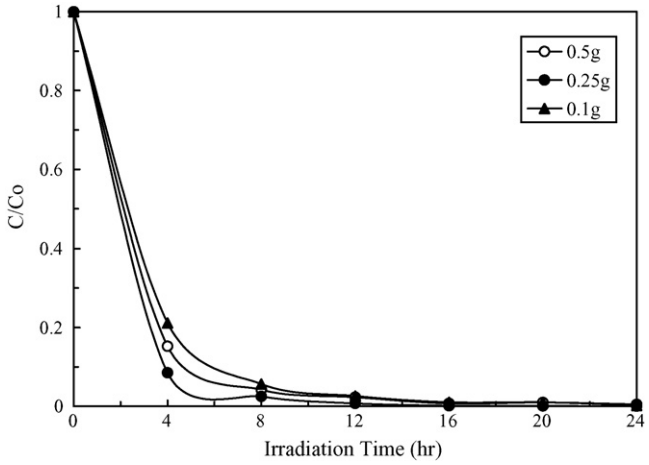

Fig. 3. Influence of the catalyst concentration on the photodegradation rate for the decomposition of MG. Experimental conditions: dye concentration (0.05 g L^{-1}), pH 7, absorbance was recorded at 620 nm, continuous stirring, irradiation time as 24 h.

easily under pH > pHzpc (zero point charge) conditions while in the reverse condition it would adsorb anionic ones. However, the adsorption of the substrate onto the TiO_2 surface directly affects the occurrence of electron transfer between the excited dye and TiO_2 and further influences the degradation rate. The surface becomes positively charged, and the number of adsorption sites may decrease above the isoelectric point of TiO_2. A similar effect of the pH on the adsorption and photocatalytic reaction has been reported for Ag deposition [17] and the degradation of formic acid [18].

The photodegradation rate of the MG dye as a function of reaction pH is shown in Fig. 2. This rate was found to increase along with increases in pH. Under acidic conditions, it was difficult for cationic MG dye to adsorb onto the TiO_2 surface. With the active $^{\bullet}OH$ radicals usually in low concentrations, the photodegradation of MG remained very slow. With higher pH values, the formation of active $^{\bullet}OH$ species is favored, due not only to improved transfer of holes to the adsorbed hydroxyls, but also to electrostatic abstractive effects between the negatively charged TiO_2 particles and the operating cationic dyes. Although the MG dye can adsorb onto the TiO_2 surface to some extent in alkaline media, when the pH value is too high (pH 11), the MG dye molecules will change to a leuco compound. In a good agreement with the adsorption mechanism proposed in Ref. [19], our results indicate that the TiO_2 surface is negatively charged, and the MG adsorbs onto the TiO_2 surface through the positive ammonium groups.

3.2. Effect of photocatalyst concentration

From both a mechanistic and an application point of view, studying the dependence of the photocatalytic reaction rate on the concentration of TiO_2 in the MG dye is important. Hence, the effect of photocatalyst concentration on the photodegradation rate of the MG dye was investigated by employing different concentrations of TiO_2 varying from 0.1 to 0.5 g L^{-1}. As expected, the photodegradation rate of the MG was found to increase, then decrease with the increase in the catalyst concentration (Fig. 3), a general characteristic of heterogeneous photocatalyst, and our results are in agreement with the earlier reports [2]. From Fig. 3, it is clear that dye degradation is faster for TiO_2 dose 0.25 g L^{-1}, then 0.5 and 0.1 g L^{-1}. This phenomenon may be due to the aggregation of TiO_2 particles at high concentrations (0.5 g L^{-1}) causing a decrease in the number of surface active sites. It is known, however, that the scattering light has a practical limit when using high concentration of TiO_2 particles, above which the degradation rate will decrease due to the reduction of the photonic flux within the irradiated solution.

3.3. Effect of dye concentration

In the typical textile effluent, dye concentration ranges from 0.15 to 0.2 g L^{-1}. By varying the initial concentration from 0.05 to 0.25 g L^{-1} at constant catalyst loading (0.25 g L^{-1}, pH 9), its effect on the degradation rate could be determined, and the results are shown in Fig. 4. As seen in the figure, degradation efficiency is inversely affected by the dye concentration. This negative effect can be explained as follows; as the dye concentration is increased, the equilibrium adsorption of dye on the catalyst surface active sites increases; hence competitive

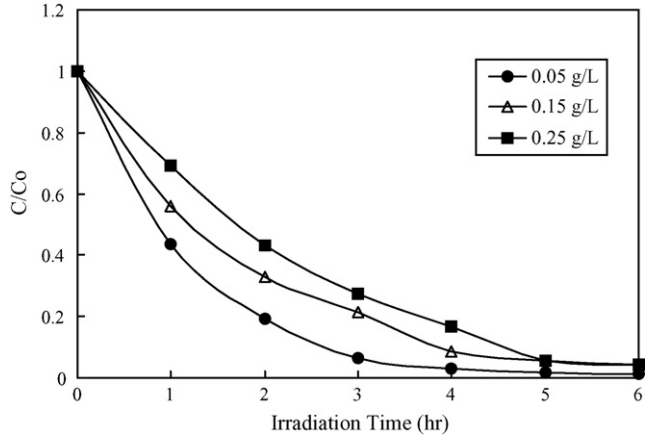

Fig. 4. Influence of initial dye concentration on the photodegradation rate for the decomposition of MG.

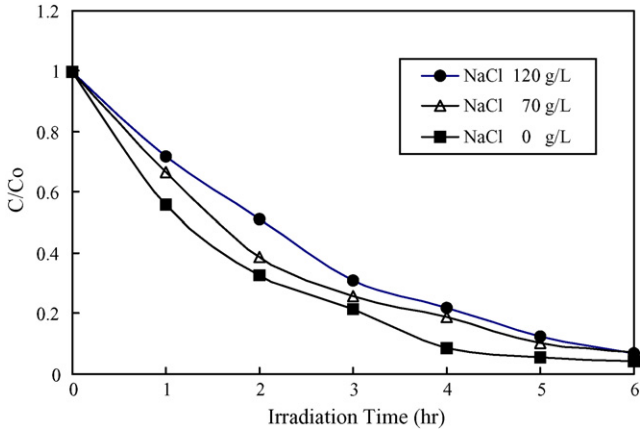

Fig. 5. Influence of NaCl concentration on the photodegradation rate for the decomposition of MG.

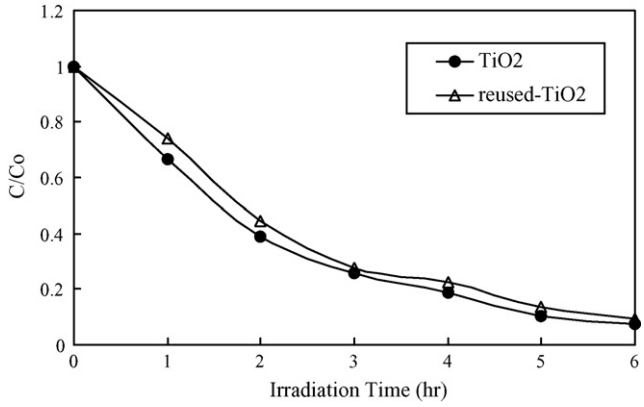

Fig. 6. Comparison of degradation rate for the decomposition of MG under TiO_2 and reused-TiO_2.

adsorption of OH^- on the same sites decreases, meaning a lower formation rate of $^{\bullet}OH$ radical, which is the principal oxidant necessary for a high degradation efficiency. On the other hand, considering the Beer–Lambert law, as the initial dye concentration increases, the path length of photons entering the solution decreases, resulting in lower photon adsorption on catalyst particles and, consequently, a lower photodegradation rate.

3.4. Effect of NaCl

In the typical textile effluent, about 70–120 g L^{-1} of NaCl is present. The role of NaCl on the degradation rate was studied at a pH of 9, a dye concentration of 0.15, 0.25 g L^{-1} TiO_2 catalyst loading, and an irradiation time of 6 h. The results in Fig. 5 show that the rate of degradation slightly decreases with increasing NaCl concentration. Inhibition effects of anions can be explained as the reaction of positive holes and hydroxyl radical with anions that behaved as h_{vb}^+ and $^{\bullet}OH$ radical scavengers (Eqs. (1) and (2)) resulting in prolonged color removal. Probably, the adsorbed anions compete with MG dye for the photo-oxidizing species on the surface and prevent the photocatalytic degradation of the dyes. Formation of inorganic radical anions (e.g. $Cl^{\bullet}$, $ClOH^{\bullet -}$) under these circumstances is possible.

$$Cl^- + h_{vb}^+ \rightarrow Cl^{\bullet} \quad (1)$$

$$Cl^- + {}^{\bullet}OH \rightarrow ClOH^{\bullet -} \quad (2)$$

Although the reactivity of these radicals may be considered, they are not as reactive as h_{vb}^+ and $^{\bullet}OH$, and thus the observed retardation effect is still thought to be the strong adsorption of the anions on the TiO_2 surface [20].

3.5. Comparison of TiO_2 and reused-TiO_2 degradation efficiencies

Initially, the experiments were performed under UV irradiation with the addition of a TiO_2 catalyst, and the photodegradation efficiency was observed. To compare the efficiency, reused-TiO_2 catalyst was tried under the same process conditions. Typical results are shown in Fig. 6 at dye concentration = 0.15 g L^{-1}, pH 9, NaCl concentration = 70 g L^{-1}, catalyst loading = 0.25 g L^{-1}, and irradiation time = 6 h. They show that reused-TiO_2 catalyst exhibits lower photocatalytic activity than the TiO_2 catalyst, and the explanation is that as the surface active sites of reused-TiO_2 catalyst decrease, the equilibrium adsorption of dye and adsorption of OH^- on the catalyst surface active sites also decrease, which means a lower degradation efficiency.

3.6. UV–vis spectra

The aqueous solution of the MG dye was a little unstable under UV radiation in absence of TiO_2. However, the MG dye can be degraded efficiently in aqueous MG/TiO_2 dispersions by UV irradiation at a wavelength of 365 nm. The changes of the UV–vis spectra during the photodegradation process of the MG dye in the aqueous TiO_2 dispersions under UV irradiation are illustrated in Fig. 7. After UV irradiation for 4 h, ca. 99.9% of the MG dyes was degraded.

During UV irradiation, at pH 3, the characteristic absorption band of the dye around 620.1 nm decreased rapidly, but no hypsochromic shifts appeared. It may indicate the photodegradation mechanism is favorable to cleavage of the whole conjugated chromophore structure of the MG dye (Fig. 7a). It was also found that the absorbance decreased from 0.70 to 0.62 AU—the former was in the initial dye concentration while the latter was added 0.05 g TiO_2 to 100 mL solution. The result showed that the cationic dye MG was difficult to adsorb on the TiO_2 surface and hence the photodegradation efficiency was slow.

At pH 7, the characteristic absorption band of the dye around 620.1 nm decreased rapidly with slight hypsochromic shifts (599.3 nm), but no new absorption bands appeared even in the ultraviolet range ($\lambda > 200$ nm), which indicated that a series of *N*-de-methylated intermediates may have formed and the whole conjugated chromophore structure of the MG dye (Fig. 7b) may have been cleaved. It was also observed that the absorbance from 0.43 to 0.15 AU—the former was in the initial dye concentration while the latter was added 0.05 g TiO_2 to 100 mL solution. The result showed that the cationic dye MG can adsorb on the TiO_2 surface in middle media and therefore the photodegradation of MG was faster.

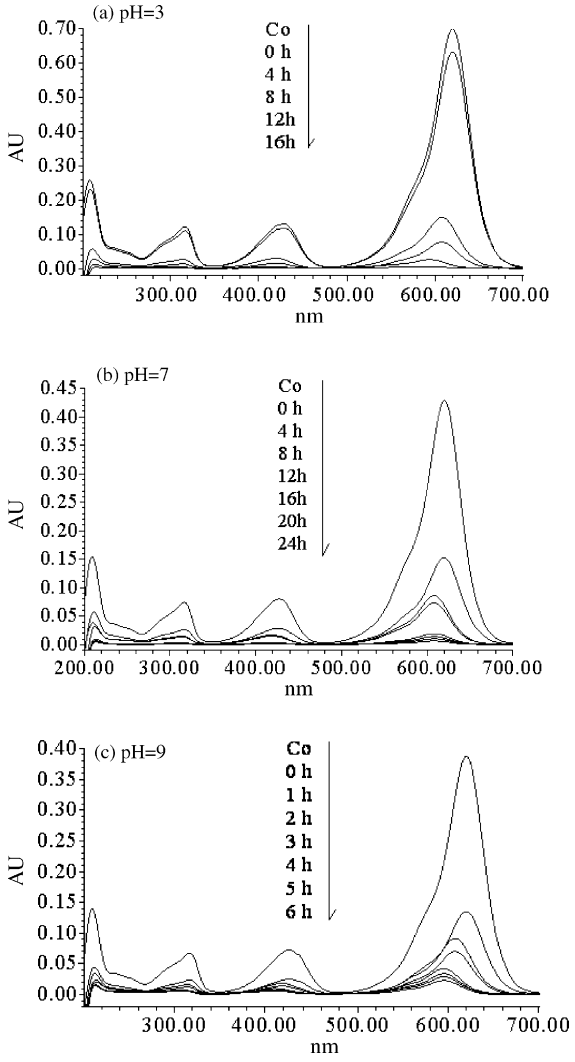

Fig. 7. UV–vis spectra changes of the MG dye in aqueous TiO_2 dispersions (MG 0.05 g L^{-1}, TiO_2 0.5 g L^{-1}) as a function of the irradiation time at different pH values. Co is initial dye concentration, without addition of TiO_2 to solution.

At pH 9, the characteristic absorption band of the dye around 620.1 nm decreased rapidly with the hypsochromic shifts (596.3 nm), but no new absorption bands appeared even in the ultraviolet range ($\lambda > 200$ nm), which indicated that there might be favor a formation of series of *N*-de-methylated intermediates of the MG dye (Fig. 7c). It was examined that the absorbance decreased quickly from 0.39 to 0.13 AU—the former was in the initial dye concentration while the latter was added 0.05 g TiO_2 to 100 mL solution. The result demonstrated that the cationic dye

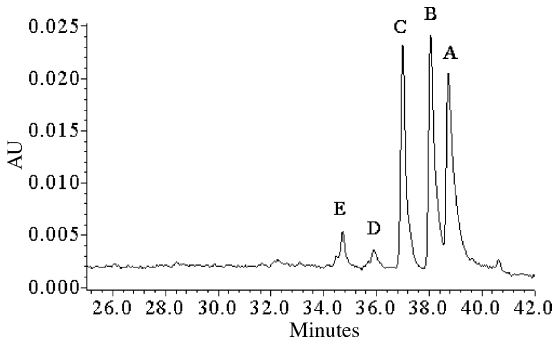

Fig. 8. HPLC chromatogram of the *N*-de-methylated intermediates with 12 h of irradiation, recorded at 620 nm.

MG can easily adsorb on TiO_2 surface to some extent in alkaline media and therefore the TiO_2-assisted photodegradation of MG was the fastest of the three. Further irradiation caused the decrease of the absorption band at 596.3 nm, but no further wavelength shift was observed, allowing us to infer that the band at 596.3 nm might be that of the full *N*-de-methylated product of the MG dye.

3.7. Separation and identification of the intermediates

Temporal variations occurring in the MG dye solution during the photodegradation process with UV irradiation were examined with HPLC, coupled with a photodiode array detector, and ESI mass spectrometry. The relevant change in the chromatograms recorded at 620 nm is illustrated in Fig. 8. With irradiation up to 12 h, five components are identified, all with retention times less than 42 min. We denoted the MG dye and

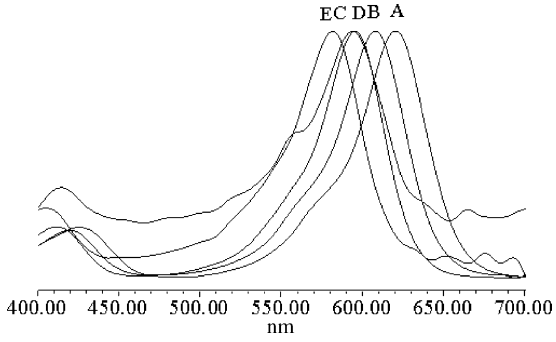

Fig. 9. Absorption spectra of the *N*-de-methylated intermediates formed during the photodegradation process of the MG dye corresponding to the peaks in the HPLC chromatograph of Fig. 8. Spectra were recorded using the photodiode array detector. Spectra A–E correspond to the peaks A–E in Fig. 8, respectively.

Table 1
Identification of the *N*-de-methylation intermediates of the MG dye by HPLC–ESI-MS

HPLC peaks	*N*-De-methylation intermediates	Abbreviation	ESI-MS peaks (*m*/*z*)	Absorption maximum (nm)
A	Bis(*p*-dimethylaminophenyl)phenylmethylium	DD-PM; MG	329.26	620.1
B	(*p*-Dimethylaminophenyl) (*p*-methylaminophenyl)phenylmethylium	DM-PM	315.18	607.9
C	(*p*-Methylaminophenyl) (*p*-methylaminophenyl)phenylmethylium	MM-PM	301.22	598.1
D	(*p*-Dimethylaminophenyl) (*p*-aminophenyl)phenylmethylium	D-PM	301.22	599.0
E	(*p*-Methylaminophenyl) (*p*-aminophenyl)phenylmethylium	M-PM	287.08	589.6
F	Bis(*p*-aminophenyl)phenylmethylium	PM	N/A	N/A

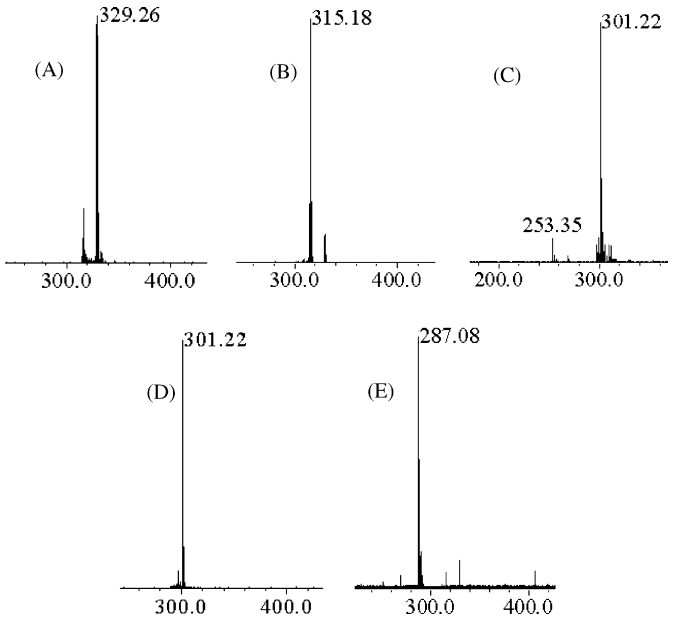

Fig. 10. ESI mass spectra of *N*-de-methylated intermediates formed during the photodegradation of the MG dye after they were separated by HPLC method: mass spectra denoted A–E corresponds to the A–E species in Fig. 8, respectively.

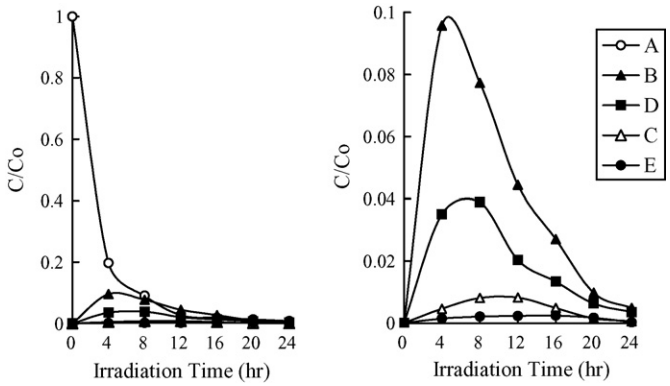

Fig. 11. Variation in the relative distribution of the *N*-de-methylated products obtained from the photodegradation of the MG dye as a function of the irradiation time. Curves A–E corresponds to the peaks A–E in Fig. 8, respectively.

its related intermediates as species A–E. Except for the initial MG dye (peak A), the intensities of the other peaks increased at first and subsequently decreased, indicating the formation and transformation of the intermediates. The absorption spectra of each intermediate in the visible spectral region are depicted in Fig. 9. They are identified as A–E (Fig. 9), corresponding to the peaks A–E in Fig. 8, respectively. The absorption maximum of the spectral bands shifts hypsochromically from 620.1 nm (Fig. 9, spectrum A) to 589.6 nm (Fig. 9, spectrum E). For example, λ_{max} of A–E are 620.1, 607.9, 598.1, 599.0 and 589.6 nm, respectively. This hypsochromic shift of the absorption band is presumed to result from the formation, in a stepwise manner, of a series of *N*-de-methylated intermediates. Similar phenomena were also observed during the photodegradation of rhodamine-B [21,22] and sulforhodamine-B [1] under visible irradiation.

As depicted in Fig. 9, the wavelength shifts are due to the *N*-de-methylation of the MG dye caused by the attacks of some active oxygen species on the *N*,*N*-dimethyl and *N*-methyl groups. Examination of the spectral variation of Fig. 7c suggests that the MG dye is *N*-de-methylated in a stepwise manner (i.e., methyl groups are removed one by one as confirmed by the gradual peak wavelength shifts toward the blue region). The wavelengths of the major absorption peaks for the *N*-de-methylated MG products are all found with a blue shift with respect to the wavelength of MG. The results are summarized in Table 1. During the initial period of MG dye photodegradation, competitive reactions between *N*-de-methylation and cleavage of the MG chromophore ring structure occur, however, with each predominating at a different pH value.

The *N*-de-methylated intermediates were further identified using the HPLC–ESI mass spectrometric method, and the relevant mass spectra are illustrated in Fig. 10. The molecular ion peaks appeared to be in the acid forms of the intermediates. From the results of mass spectral analysis, we confirmed that the component A, $m/z = 329.26$, in the liquid chromatogram is MG (Fig. 7, mass spectra A). The other components are B, $m/z = 315.18$, (*p*-dimethylaminophenyl)(*p*-methylaminophenyl)phenylmethylium (Fig. 7, mass spectra B); C, $m/z = 301.22$, (*p*-dimethylaminophenyl) (*p*-aminophenyl) phenylmethylium (Fig. 7, mass spectra C); D, $m/z = 301.22$, (*p*-methylaminophenyl)(*p*-methylaminophenyl)phenylmethylium (Fig. 7, mass spectra D); E, $m/z = 287.08$, (*p*-methylaminophenyl) (*p*-aminophenyl)phenylmethylium (Fig. 7, mass spectra E). Results of HPLC chromatograms, UV–vis spectra, and HPLC–ESI mass spectra are summarized in Table 1.

However, the emerging intermediates, the absorption-maximum peaks of which can be easily observed in Fig. 11, correspond to those species with several methyl groups detached from the MG dye. According to the number of the methyl groups detached, we can characterize these intermediates. We have found a pairs of isomeric molecules, i.e., di-*N*-de-methylated MG species, different only in the way the methyl groups are released from the benzyl groups. One of the di-*N*-de-methylated MG isomers, MM-PM, is formed by the removal of a methyl group from two different benzyl groups of the MG molecule while the other isomer, D-PM, is produced by releasing two methyl groups from the same benzyl group of the MG dye. Therefore, considering the polarity of the D-PM species is greater than that of the MM-PM intermediates, we expected the latter to be eluted first. As well, to the extent that two *N*-methyl groups are stronger auxochromic moieties than the *N*,*N*-dimethyl groups and amino group are, the maximal absorption of the D-PM intermediates was anticipated to occur at wavelengths shorter than the band position of the MM-PM species. This argument will be supported by the following results and a mechanism is proposed accordingly.

The relative distribution of the *N*-de-methylated intermediates obtained is illustrated in Fig. 11. To minimize errors, the relative intensities were recorded at the maximum absorption wavelength for each intermediate, although a quantitative determination of all of the photogenerated intermediates was not achieved, owing to the lack of the appropriate molar extinction coefficients of these intermediates and the related reference

standards. The distributions of all of the *N*-de-methylated intermediates are relative intermediates with the initial concentration of MG. Nonetheless, we clearly observed the changes in the distribution of each intermediate during the photodegradation process of the MG dye. In accordance with the data of Fig. 11, the successive appearance of the maximal distribution of each intermediate indicates that the *N*-de-methylation of MG is a stepwise photochemical process.

According to earlier reports [23–25], most oxidative *N*-dealkylation processes are preceded by the formation of a nitrogen-centered radical, but the destruction of the dye chromophore structures is preceded by the generation of a carbon-centered radical [3,26,27]. To be consistent with the above statement, the degradation of MG must occur via two different photooxidation pathways (destruction of the chromophore structure and *N*-de-methylation) due to the formation of the different radicals (either carbon-centered radical or nitrogen-centered radical). There is no doubt that electron injection from the dye to the positive holes of TiO_2 yields the dye cationic radical. After this stage, the cationic radical, $Dye^{\bullet+}$, can undergo hydrolysis and/or deprotonation pathways of the dye cationic radicals, which in turn are determined by the different adsorption modes of MG on the TiO_2 particles surface [28].

When the MG dye molecules are located near the TiO_2 surface due to the dimethylamine group, which somewhat neutralizes the surface, the *N*-de-methylation process predominates during the initial stages. Destruction of the chromophore ring structure occurs mostly only after full *N*-de-methylation of the dye occurs.

Under UV irradiation, most of the $^{\bullet}OH$ radicals are generated directly from the reaction between the holes and surface-adsorbed H_2O or OH^-. The probability for the formation of $O_2^{\bullet-}$ should be much less than for $^{\bullet}OH$ [22]. The *N*-de-methylation of the MG dye occurs mostly by the attack of the $^{\bullet}OH$ species on the *N*,*N*-dimethyl groups of the MG dye. Considering that the *N*,*N*-dimethyl group in D-PM is bulkier than the *N*-methyl group in MM-PM molecules, the attack of $^{\bullet}OH$ radicals on the *N*-methyl groups should be favored at the expense of the *N*,*N*-dimethyl groups. In accord with this notion, the HPLC results showed that the D-PM intermediates reached maximal concentration before the MM-PM intermediates did. The *N*-di-demethylated intermediates (MM-PM and D-PM) were clearly observed (Fig. 11, curve C–D) to reach their maximum concentrations after 12- and 8-h irradiation periods due to the factor mentioned above. The *N*-tri-demethylated intermediates (M-PM) were clearly observed (Fig. 11, curve E) to reach their maximum concentration after a 16-h irradiation period because the $^{\bullet}OH$ attacked the *N*-methyl groups of MM-PM and the *N*,*N*-dimethyl group of D-PM. The successive appearance of the maximal quantity of each intermediate indicates that the *N*-de-methylation of MG is a stepwise photochemical process occurring by a dehydroxylation of *N*-hydroxymethylated intermediates. The results discussed above can be seen more clearly from Scheme 1.

The *N*-mono-demethylated intermediates (DM-PM) were clearly observed (Fig. 11, curve B), following which DM-PM degraded rapidly. A small amount of the fourth *N*-de-methylated intermediate (PM) was not detected. The first product (DM-PM) of *N*-de-methylation reached its maximum concentration after a 4-h irradiation period (Fig. 11, curve B) while the maximum of the third *N*-de-methylated product (M-PM) appeared after a 24-h irradiation (Fig. 11, curve E). The chromophoric species (MG) was still observed even after irradiation for 24 h. This indicates that the *N*-de-methylation process predominates, and the cleavage of the conjugated structure occurs at a somewhat slower rate until all four methyl groups are removed.

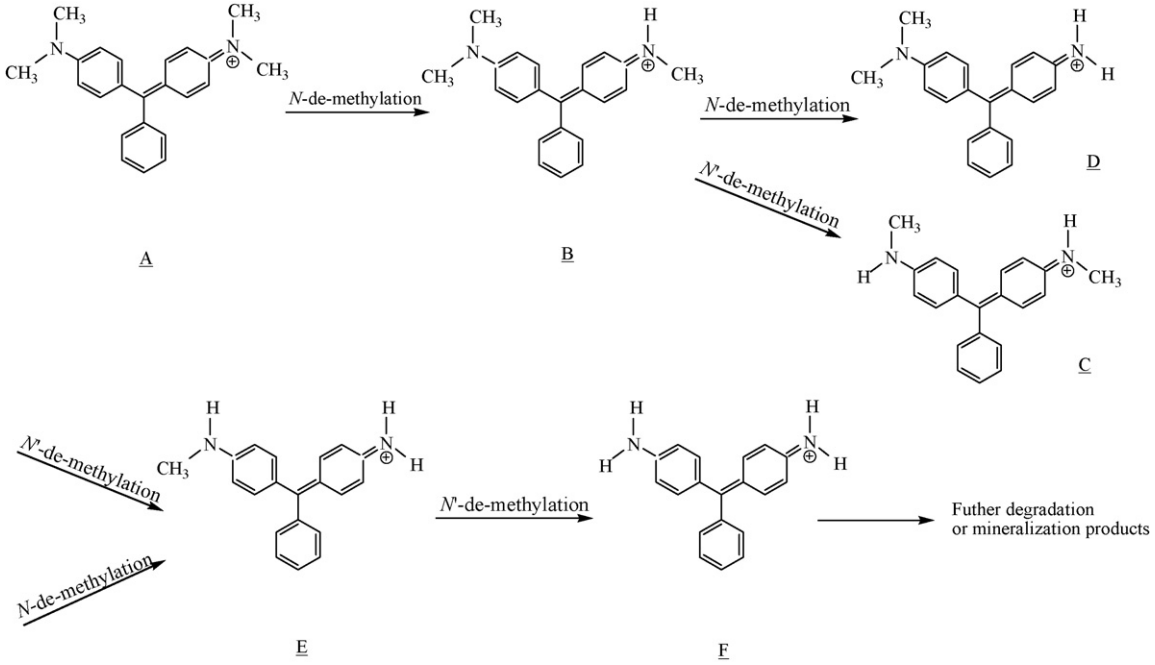

Scheme 1. Proposed *N*-de-methylation mechanism of the MG dye under UV irradiation in aqueous TiO_2 dispersions followed by the identification of several intermediates by HPLC-ESI mass spectral techniques.

On the basis of all the above experimental results, we tentatively propose the pathway of demethylation as depicted in Scheme 1. The dye molecule in the MG/TiO_2 system is adsorbed through the positively charged dimethylamine groups. Then the $^{\bullet}OH$ radicals are attacked from the TiO_2 particle surface to the adsorbed dye through the positively charged dimethylamine groups. The subsequence hydrolysis (or deprotonation) yields a nitrogen-centered radical, which is then attacked by molecular oxygen to lead ultimately to de-methylation. The mono-de-methylated dye, DM-PM, can also be adsorbed on the TiO_2 particle surface and be involved in the other similar events (such as $^{\bullet}OH$ attack, oxygen attack and hydrolysis, or deprotonation) to yield a bi-de-methylated dye derivative, D-PM and MM-PM. The de-methylation process described above continues until formation of the completely de-methylated dye, PM.

4. Conclusion

The photodegradation rate of MG dye was found to increase along with increasing pH and was found to increase then decrease along with increasing catalyst concentration. After 15 W UV-365 nm irradiation for 4 h, ca. 99.9% of MG was degraded. The MG dye could be successfully decolorized and degraded by TiO_2 under UV irradiation.

Under acidic conditions, the result indicated that the photodegradation mechanism is favorable to cleavage of the whole conjugated chromophore structure of the MG dye, the cationic dye MG was difficult to adsorb on the TiO_2 surface, and hence the photodegradation efficiency was slow. Under basic conditions, the results showed that the photodegradation mechanism is favorable to a formation of a series of *N*-de-methylated intermediates of the MG dye, the cationic dye MG can easily adsorb on TiO_2 surface to some extent in alkaline media, and therefore the TiO_2-assisted photodegradation of MG was faster. Both *N*-de-methylation and degradation of the MG dye take place in the presence of TiO_2 particles.

The *N*-de-methylation of the MG dye takes place in a stepwise manner with the various *N*-de-methylated intermediate MG species. The *N*-de-methylation process continues until formation of the completely *N*-de-methylated dye. In addition, the methyl groups are removed one by one as confirmed by the gradual wavelength shifts of the maximum-peaks toward the blue region. The hypsochromic effects resulting from *N*-de-methylated intermediates of the MG dye occurred concomitantly during irradiation. The photodegradation mechanisms of TiO_2/UV proposed in this study may shed some light on future applications of the technology for the decoloration of dyes.

References

[1] C.C. Chen, W. Zhao, J.G. Li, J.C. Zhao, H. Hidaka, N. Serpone, Formation and identification of intermediates in the visible-light-assisted photodegradation of sulforhodamine-B dye in aqueous TiO_2 dispersion, Environ. Sci. Technol. 36 (2002) 3604–3611.

[2] M. Saquib, M. Muneer, TiO_2-mediated photocatalytic degradation of a triphenylmethane dye (gentian violet), in aqueous suspensions, Dyes Pigment. 56 (2003) 37–49.

[3] H. Kyung, J. Lee, W. Choi, Simultaneous and synergistic conversion of dyes and heavy metal ions in aqueous TiO_2 suspensions under visible-light illumination, Environ. Sci. Technol. 39 (2005) 2376–2382.

[4] A.L. Linsebigler, G.Q. Lu, J.T. Yates Jr., Phtocatalysis on TiO_2 surfaces: principles, mechanisms, and selected results, Chem. Rev. 95 (1995) 735–758.

[5] M.R. Hoffman, S.T. Martin, W. Choi, W. Bahnemann, Environmental applications of semiconductor photocatalysis, Chem. Rev. 95 (1995) 69–96.

[6] R.A. Schnick, The impetus to register new therapeutants for aquaculture, Prog. Fish Cult. 50 (1998) 190–196.

[7] S. Srivaji, R. Sinha, D. Roy, Toxicological effects of malachite green, Aquat. Toxicol. 66 (2004) 319–329.

[8] S.J. Culp, F.A. Beland, Malachite green: a toxicological review, J. Am. Coll. Toxicol. 15 (1996) 219–238.

[9] D.J. Alderman, R.S. Clifton-Hadley, Malachite green: a pharmacokinetic study in rainbow trout, Oncorhynchus mykiss (Walbaum), J. Fish Dis. 16 (1993) 297–311.

[10] A.A. Bergwerff, P. Scherpenisse, Determination of residues of malachite green in aqueous animals, J Chromatogr. B 788 (2003) 351–359.

[11] S.J. Culp, F.A. Beland, R.H. Heflich, R.W. Benson, L.R. Blankenship, P.J. Webb, P.W. Mellick, R.W. Trotter, S.D. Shelton, K.J. Greenlees, M.G. Manjanatha, Mutagenicity and carcinogenicity in relation to DNA adduct formation in rats fed Leucomalachite green, Mutat. Res. 506/507 (2002) 55–63.

[12] C.R. Nelson, R.A. Hites, Aromatic amines in and near the buffalo river, Environ. Sci. Technol. 14 (1980) 147–149.

[13] J. Zhao, K. Wu, T. Wu, H. Hidaka, N. Serpone, Photodegradation of dyes with poor solubility in an aqueous surfactant/TiO_2 dispersion under visible light irradiation, J. Chem. Soc. Faraday Trans. 94 (1998) 673–676.

[14] H. Kominami, H. Kumamoto, Y. Kera, B. Ohtani, Photocatalytic decolorization and mineralization of malachite green in an aqueous suspension of titanium (IV) oxide nano-particles under aerated conditions: correlation between some physical properties and their photocatalytic activity, J. Photochem. Photobiol. A: Chem. 160 (2003) 99–104.

[15] Y. Bessekhouad, D. Robert, J.V. Weber, Synthesis of photocatalytic TiO_2 nanoparticles: optimization of the preparation conditions, J. Photochem. Photobiol. A: Chem. 157 (2003) 47–53.

[16] J. Zhao, H. Hidaka, A. Takamura, E. Pelizzetti, N. Serpone, Photodegradation of surfactants. 1. Zeta-potential measurements in the photocatalytic oxidation of surfactants in aqueous titania dispersions, Langmuir 9 (1993) 1646–1650.

[17] B. Ohtani, Y. Okugawa, S. Nishimoto, T. Kagiya, Photocatalytic activity of titania powders suspended in aqueous silver nitrate solution: correlation with pH-dependent surface structures, J. Phys. Chem. 91 (1987) 3550–3555.

[18] D.H. Kim, M.A. Anderson, Solution factors affecting the photocatalytic and photoelectrocatalytic degradation of formic acid using supported TiO_2 thin films, J. Photochem. Photobiol. A: Chem. 94 (1996) 221–229.

[19] X. Li, G. Liu, J. Zhao, Two competitive primary processes in the photodegradation of cationic triarylmethane dyes under visible irradiation in TiO_2 dispersions, New J. Chem. 23 (1999) 1193–1196.

[20] M. Sökmen, A. Özkan, Decolourising textile wastewater with modified titania: the effects of inorganic anions on the photocatalysis, J. Photochem. Photobiol. A: Chem. 147 (2002) 77–81.

[21] J. Zhao, T. Wu, K. Wu, K. Oikawa, H. Hidaka, N. Serpone, Photoassisted degradation of dye pollutants. 3. Degradation of the cationic dye rhodamine B in aqueous anionic surfactant/TiO_2 dispersions under visible light irradiation: evidence for the need of substrate adsorption on TiO_2 particles, Environ. Sci. Technol. 32 (1998) 2394–2400.

[22] T. Wu, G. Liu, J. Zhau, H. Hidaka, N. Serpone, Photoassisted degradation of dye pollutants. V. Self-photosensitized oxidative transformation of rhodamine B under visible light irradiation in aqueous TiO_2 dispersions, J. Phys. Chem. B 102 (1998) 5845–5851.

[23] G. Galliani, B. Rindone, C. Scolastico, Selective de-methylation in the oxidation of arylalkylmethylamines with metal acetates, Tetrahedron Lett. (1975) 1285–1288.

[24] F.C. Shaefer, W.D. Zimmermann, Dye-sensitized photochemical autoxidation of aliphatic amines in non-aqueous media, J. Org. Chem. 35 (1970) 1970–2165.

[25] B.L. Laube, M.R. Asirvatham, C.K. Mann, Electrochemical oxidation of tropanes, J. Org. Chem. 42 (1977) 670–674.

[26] G. Liu, T. Wu, J. Zhao, K. Wu, K. Oikawa, H. Hidaka, N. Serpone, Photocatalytic degradation of dye sulforhodamine B: a comparative study of photocatalysis with photosenitization, New J. Chem. 24 (2000) 411–417.

[27] G. Liu, J. Zhao, K. Wu, K. Oikawa, H. Hidaka, N. Serpone, Photoassisted degradation of dye pollutants. 8. Irreversible degradation of alizarin red under visible light radiation in air-equilibrated aqueous TiO_2 dispersions, Environ. Sci. Technol. 33 (1999) 2081–2087.

[28] G. Liu, X. Li, J. Zhao, H. Hidaka, N. Serpone, Photooxidation pathway of sulforhodamine-B. Dependence on the adsorption mode on TiO_2 exposed to visible light radiation, Environ. Sci. Technol. 34 (2000) 3982–3990.